Local Nusselt number and temperature field in turbulent flow through a heated square-sectioned U-bend

R. W. Johnson and B. E. Launder*

Local heat transfer coefficients and temperature distributions within the fluid for air flow around a 180° square-sectioned bend have been measured. The ratio of bend radius to hydraulic diameter of the duct is 3.35:1 and the flow entering the bend is sensibly fully developed. Measurements of air and wall temperatures span a range of Reynolds numbers from 9.9×10^3 to 9.2×10^4 with the principal emphasis given to the case of $Re \simeq 5.6 \times 10^4$. This Reynolds number and geometric configuration coincide with that of a companion LDA study carried out by Chang *et al*[1] which provides detailed maps of the mean and turbulent velocity fields. The data show that by 45° into the bend the heat transfer coefficients on the inner convex wall of the bend drop markedly while those on the other walls increase. By 90° the ratio of the heat transfer coefficients at the mid positions of the concave and convex walls is more than 2:1. Nevertheless this ratio is less than would be anticipated from considering two-dimensional flow on weakly curved surfaces. There is a general consistency between the velocity and the temperature field data in the heated fluid

Keywords: *turbulence, ducting, heat transfer, convection*

Turbulent flows through the passages of turbine blades and stators are complex examples of turbulent duct flows with strong streamline curvature and substantial secondary flow. Even weak streamline curvature has a remarkably strong effect on the turbulence structure in wall turbulence[2] with consequent effects on the prevailing levels of heat transfer coefficient[3,4]. Likewise, even the weak secondary flows generated by the anisotropic turbulent stress field in straight square ducts[5], at most of the order of 1% of the streamwise mean velocity, are known to produce a substantial modification in the perimetral distribution of heat transfer coefficient[6,7].

In strongly curved ducts such as arise in various hot section components of gas turbines, both streamline curvature and secondary flow levels may be more than an order of magnitude larger than those produced in the experiments cited above. Several flow-field studies at Imperial College, London, UK, have provided quantitative data on the development of the secondary motion and turbulence field in 90° square-sectioned bends[8-10], but little is known about the effects of these developments on the temperature field and surface heat transfer coefficients. The only published measurement of semi-local† heat transfer coefficients in curved rectangular ducts appear to be the recent data of Metzger and Larsen[11]. These show a maximum circumferential variation of Nusselt number of 170% with the maximum and minimum heat transfer coefficients occurring on the concave and convex walls of the bend respectively.

In general, knowledge of convective heat transfer in complex turbulent flows is hampered by the absence of flow-field data. Experimental difficulties often preclude complete mapping, but some exploration of the mean and turbulent flow distributions is essential if the heat transfer behaviour is to be understood. The experiments reported here aimed to provide an extensive set of data of convective heat transfer in turbulent flow around a 180° bend of square cross-section. This flow does not contain the leading edge horseshoe vortex present in stator-passage flows, but does exhibit other features such as strong curvature and secondary flow and is, therefore, important in developing an understanding of convective heat transfer in blade passages. Although only limited velocity field data were acquired, the project was undertaken in close collaboration with Professor J. A. C. Humphrey and his group[1] at UC Berkeley, USA, who have reported data of the mean and turbulent velocity fields in the same geometry at the same duct Reynolds number, *Re*. Our comparisons with their measurements confirm that the flow fields produced in the two apparatuses are sensibly the same.

Apparatus, instrumentation and uncertainties

Apparatus

The test section (Fig 1) consists of a 180° bend section connecting to straight inlet and exit tangents which,

* Mechanical Engineering Department, Thermodynamics and Fluid Mechanics Division, UMIST, PO Box 88, Manchester M60 1QD, UK
Received 22 November 1984 and accepted for publication on 4 March 1985

† The mean heat transfer coefficient on each wall of the channel was determined

 0142-727X/85/030171-10$3.00

depending upon the number of sections attached, may be up to 72 hydraulic diameters in length. The cross section, 88.9 mm square, is double that of the Berkeley apparatus to facilitate matching *Re*, as the LDA study used water as the working fluid. The nominal ratio of mean bend radius to hydraulic diameter as 3.35:1, a value that provided a relatively tight bend but which did not provoke flow separation in the stream direction. The test section is constructed from 10 mm perspex sheet providing rigid, transparent walls. The side and bottom walls are permanently cemented with a perspex adhesive while the removable top wall is sealed to the side walls with soft rubber tubing inserted into grooves machined into the tops of the side walls (Fig 2). The top is clamped down onto the side walls with threaded rods. The maximum variation in the dimension of the sides of the duct is ± 0.38 mm in the straight sections and ± 0.08 mm in the bend while the walls are perpendicular within $\pm 0.2°$. The inlet and exit tangents were assembled from 1.22 m lengths of ducting joined by flanges. In the bend section the side walls are moulded to the desired shape by warming the perspex prior to bending. The outer radius of curvature was 343.1 ± 0.46 mm while that of the inner wall was 254.05 ± 0.19 mm.

At the downstream end of the exit tangent the flow passes to a section of straight PVC piping 84 diameters long at the end of which an orifice plate measures the flow rate; siting and instrumentation of the orifice plate are in accordance with BS 1042. Thereafter the air is passed to a centrifugal fan and discharged to the atmosphere through the laboratory wall. The apparatus thus operates in 'suction' mode and, at inlet, a contracting section with an

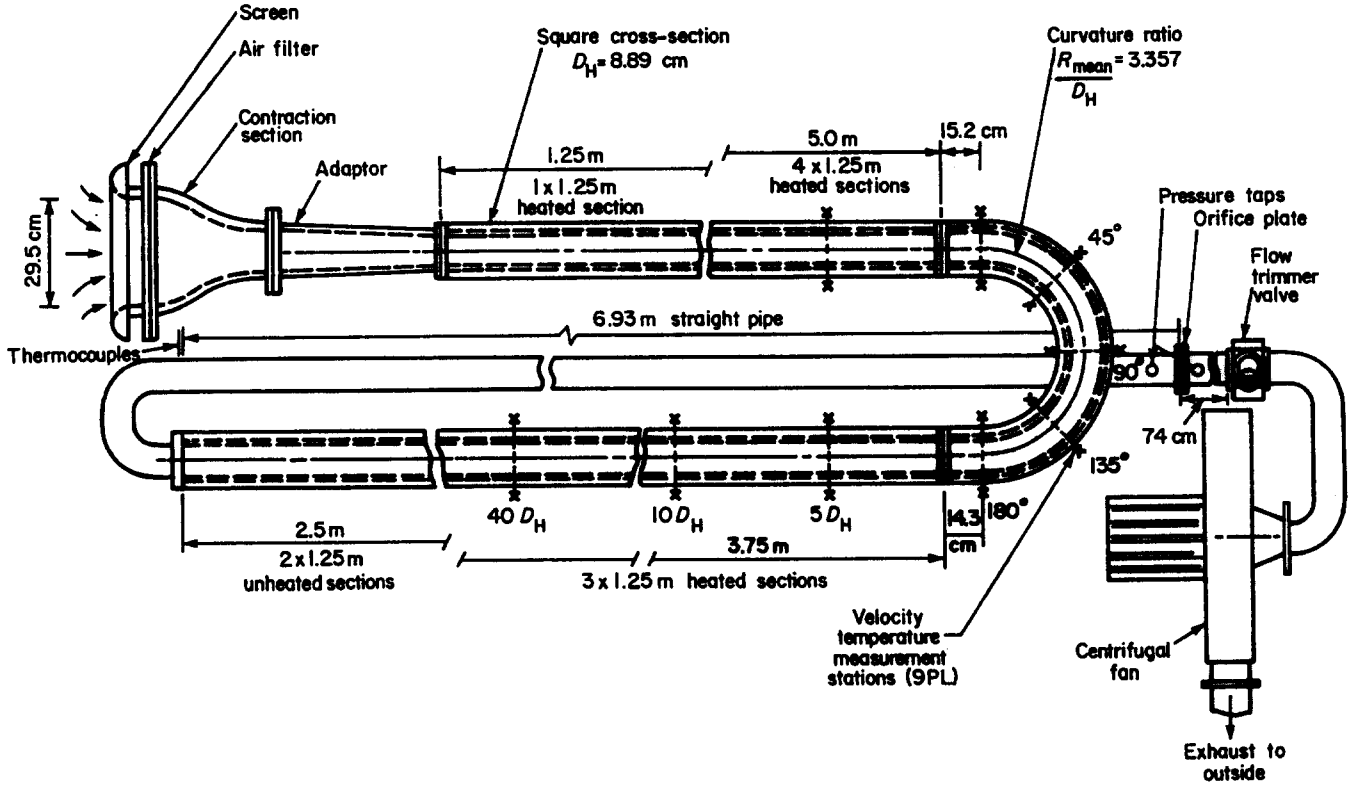

Fig 1 Apparatus with measurement stations indicated

Notation

D_H	Hydraulic diameter of cross section
k	Thermal conductivity of air
Nu	Nusselt number, $\dfrac{q''_W D_H}{(T_W - T_B)k}$
r	Radius (measured from axis passing through centre of bend and normal to plane of bend)
Re	Reynolds number based on bulk mean velocity $\bar{W}$ and D_H
r_i	Radius of inside wall of bend (R_i on computer-drawn plots)
r_o	Radius of outer wall of bend (R_o on computer-drawn plots)
T	Local temperature of air
T_B	Bulk mean temperature of air
T_W	Wall temperature
$\sqrt{\overline{w^2}}$	Root mean square streamwise turbulent velocity
W	Local streamwise velocity
$\bar{W}$	Bulk mean velocity
x	Coordinate, perpendicular to r, mapping cross section of bend with origin at lower (flat) wall
X	Dimensionless x distance (Fig 3)
Y	Dimensionless radial distance (Fig 3)
Z	Coordinate measured in flow direction (either degrees of arc around bend or distance upstream/downstream of bend)

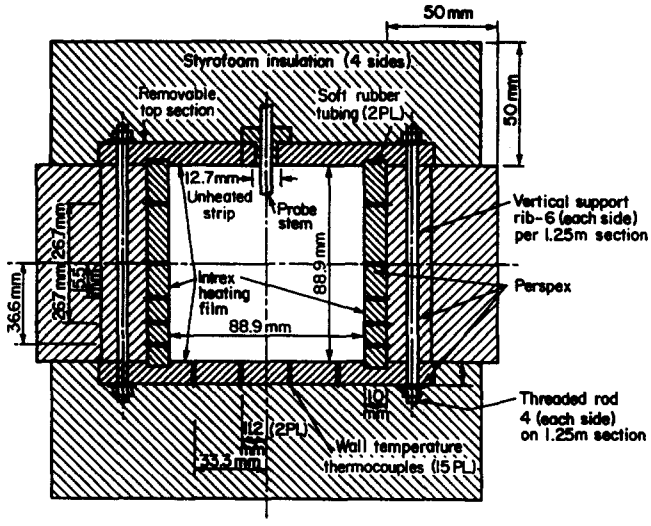

Fig 2 Cross-sectional view of square duct showing thermocouple locations

area reduction of approximately 12:1 is installed.

The experiment was one of uniform surface heat flux. Because highly non-uniform heat transfer coefficients were anticipated, the electrical heater had to be very thin to avoid substantial heat conduction within the walls. After considering various alternatives, we adopted Intrex-G‡ sheeting which had been used to measure heat-transfer coefficients in pipe flow with large circumferential variations in heat fluxes[1,2]. The material consists of a transparent polyester sheet 0.13 mm thick on one side of which a film of gold is vapour-deposited and covered by a protective film of ceramic. A precision guillotine was used to cut the Intrex into strips that were then glued to the interior walls of the duct with the gold coated surface outermost (ie exposed to the airstream). Various precautions, detailed elsewhere[1,3], were necessary to achieve a satisfactory electrical contact at the ends of the individual duct sections. The Intrex installed along the flat top and bottom walls of the bend section was scribed longitudinally into fourteen 6.35 mm wide, electrically isolated tracks, the power supply to which could be individually controlled. This feature was introduced to minimise non-uniform heating due to the difference in resistive path lengths along the inside and outside edges of the heating elements. The maximum variation of heat flux due to track curvature was thereby reduced to $\pm 2\%$.

On the top wall throughout the entire test section a 12.7 mm central section of the Intrex was left unheated because probe access for velocity and field temperature measurements was through the top plate. By leaving this central strip unheated we could avoid any variation in the heating pattern in the streamwise direction. The whole heated test section was enclosed by styrofoam sheet insulation to a depth of 50 mm. The reported thermal conductivity of this material is 0.029 W/mK. Further details are provided elsewhere[1,3].

Instrumentation

Wall temperatures were monitored with 0.2 mm diameter chromel-alumel thermocouple wire at the nine measurement stations indicated in Fig 1. At each station, 15 thermocouples were positioned as shown in Fig 2. Attention mainly focused on the half of the flow below the plane of symmetry but 3 thermocouples were included above this plane to check for symmetry and provide some indication of reproducibility of the results. The thermocouples were passed through the duct wall and cemented to the back of the Intrex sheet. Each thermocouple was coiled at the measuring junction for a distance of 10 mm (the coil being 2 mm in diameter) to reduce heat conduction along the thermocouple wire.

The air temperature within the duct was measured by a 13-prong thermocouple rake which provided a temperature profile across the width of the duct. Bottom-to-top variations in temperature were mapped by traversing the probe vertically. The horizontal support for the thermocouples was machined from Tufnol, thus eliminating any significant heat conduction between thermocouple supports. The thermocouples were made from 0.2 mm diameter PTFE chromel-alumel wire supported by 1.65 mm od stainless-steel tubes which extended 16 mm upstream of the horizontal support. The exposed junctions extended 3.3 mm ahead of the end of the stainless-steel tubes. Access holes for the rake in the top wall of the duct were positioned so that temperature profiles were obtained at the same cross-sectional planes as the wall thermocouples. The air temperature at inlet to the duct was monitored with a single thermocouple. All processing of thermocouple emf's was via a Fluke 2280A data logger.

The thermocouples, made from a continuous spool of thermocouple wire, were calibrated but only with respect to each other since only temperature differences were employed in the presentation of the data. After cutting ten successive lengths for wall thermocouples, a further 1 mm length was cut for a calibration thermocouple; a further calibration thermocouple was made from the wire used in the temperature rake. All such calibration thermocouples were exposed to a bath at room temperature and at 39°C (corresponding approximately to the upper wall temperature of the measurements). The implied difference in temperature between these bath values was less than the variation in the temperature of the aluminium block used as the reference junction in the data logger.

Fluid flow rate measurements were obtained by recording the pressure difference across standard orifice plates. Local velocities in the test section were obtained with DISA miniature hot-wire probes. A single straight wire (55P11) was used to measure the mean velocity five diameters upstream of the bend, while a crosswire probe was used in the bend itself where the secondary flows were large. In the latter case, the probe axis was pointed directly upstream with the wires parallel to the plane of symmetry of the duct. The primary mean velocity was evaluated from the signals of the two slant hot wires assuming the wire to respond only to the component normal to the wire and with negligible contribution from mean velocities at right angles to the plane of symmetry. An unlinearized ISVR hot wire anemometer was employed in these measurements.

Experimental procedures

The experiments aimed at obtaining local Nusselt number data for uniform heat flux boundary conditions. In

‡ Manufactured by the Sierracin/Sylmar Company of Sylmer, California, USA

practice, the resistivity of the Intrex sheet, even after discarding the 25% adjacent to each of the edges of the roll, exhibits variations of at least 10%. The resistivity was mapped by applying a voltage across two ends of a complete rectangular section of Intrex. A separate probe having two graphite points 12 mm apart was then used to measure the voltage drop across a short length of Intrex parallel to the current flow. The resistivity increased during actual testing. Initial ageing of less than one hour at a flux rate of 250 W/m^2 produced an increase of about 10%. Thereafter the resistance increased much more slowly to an asymptotic level of 13–15% above the original value. Based on the cold resistivity map for each wall, the trimming resistors for the straight sections were set at the start of each test to give uniform (mean) heating to each section. The mean hot resistance was about 2.5% higher than the cold value but varied somewhat from section to section and thus further minor adjustments to the individual voltage levels were applied.

A selection of wall thermocouples was used to determine when the rig had reached steady state. The criterion adopted was that all these thermocouples should change by less than 0.01°C over a 10 min period. The required warm-up times ranged from 2 h to 5 h depending on the air flow rate through the apparatus. To determine the distribution of heat transfer coefficients, the data logger was simply set in operation to record all the thermocouple voltages which were converted internally to temperature values. When obtaining air temperature data, the thermocouple rake, having been inserted and positioned prior to the start of the test, was manually stepped across the cross-section. After each movement of the rake a period of 30–60 s was allowed to elapse when no data were taken. Thereafter, the 13 thermocouples were recorded in turn by the data logger at 0.5 s intervals. This scan was repeated 5–7 times, with a 5 s interval between scans in order to form an average value of local temperature. In addition, there were about 15 planes per station so the time saving was significant since laboratory regulations allow the apparatus to be run only during the working day.

Experimental uncertainties

Johnson[13] provides a detailed assessment of uncertainties in the measurements arising from what are believed to be all the significant sources. In estimating possible errors in heat transfer coefficients, account was taken of errors in: estimating the rate of heat loss to the surroundings; determining the rate of power input; positioning thermocouples; measurement of wall and bulk fluid temperature; resistivity calibration of Intrex; conduction within the Intrex.

For the tests at medium and high Reynolds numbers, the estimated uncertainty in the resultant Nusselt numbers is 8% except as noted. At the lowest Reynolds number ($\sim 10^4$) differences between wall and bulk mean temperatures T_W and T_B became so small at certain positions on the perimeter that the resultant value of Nu became extremely sensitive to the estimated magnitude of the heat loss (since this affects T_B†). For example, from a modification in the estimated heat loss from 8 to 6.5%, a variation that was certainly within the uncertainty in our estimate of the heat loss, levels of Nu were increased at isolated points by nearly 20%.

Overall uncertainties in wall and field temperature measurements were estimated to be ±0.05°C. For most locations this represents less than ±1% of the temperature difference between wall and bulk fluid temperature (see Johnson[13], p 212).

Uncertainties in values of mean velocity were estimated at ±2% in the upstream straight section and ±3% in the bend region. The corresponding uncertainty in the rms streamwise turbulence intensity in the upstream section was ±5%. All velocity data were obtained with heating off to conform with the UC Berkeley work. In the actual heated test cases, there is typically a 2% increase in bulk mean velocity due to the decrease in average density in passage through the test section.

Scope of experimental programme

Chang *et al*[1] had documented the flow field in a U-bend with a straight entry length of 31 hydraulic diameters preceded by a flow straightening section. Accordingly, for the first experiments in our rig, only two straight duct sections were included, giving an upstream tangent length of $30D_H$. (The difference between 30 and 31 nominal hydraulic diameters development is not significant since the contraction sections were different in the two rigs.) Direct comparisons of measured velocity at two stations confirm the flow fields in the two apparatuses were essentially the same (Fig 7). For this configuration, local heat transfer coefficients were mapped at‡ $5D_H$ upstream; 0°, 45°, 90°, 135° and 180° in the bend; and at $5D_H$ and $10D_H$ downstream of the bend for a single Reynolds number of approximately 56 000. Streamwise mean velocity and turbulence intensity profiles were made $5D_H$ upstream of the bend and mean velocity only at 90°.

Since the above configuration did not provide fully-developed conditions at the entrance to the bend, further data were obtained in which all five inlet tangent duct sections were included giving a development length of $72D_H$. As the first section of this ducting was unheated, the thermal development length was $57D_H$ excluding the unheated flanges between sections. For this configuration, for a similar Reynolds number, heat transfer coefficients and flow field data were obtained at the same positions as for the earlier tests. Temperature profiles within the air were mapped at $5D_H$ upstream and 90° only. Finally, heat transfer coefficients only were obtained at the same stations as before at the highest Reynolds number obtainable with the available blower (9.2×10^4) and for a Reynolds number of approximately 10^4. Although space limitations preclude the inclusion of all these results here, a complete presentation and tabulation of the data are given by Johnson[13].

Presentation and discussion of results

Fig 3 establishes the coordinates and shows schematically the classical single-cell secondary vortex that develops

† The bulk mean temperature at any station is computed from the known entry temperature, the mass flow rate of the working fluid and the total heat supplied to this fluid

‡ These are nearly the same positions as those at which velocity data were gathered at Berkeley. Obstructions to their optical path meant that Chang *et al* made traverses at 3°, 130° and 177° rather than 0°, 135° and 180°

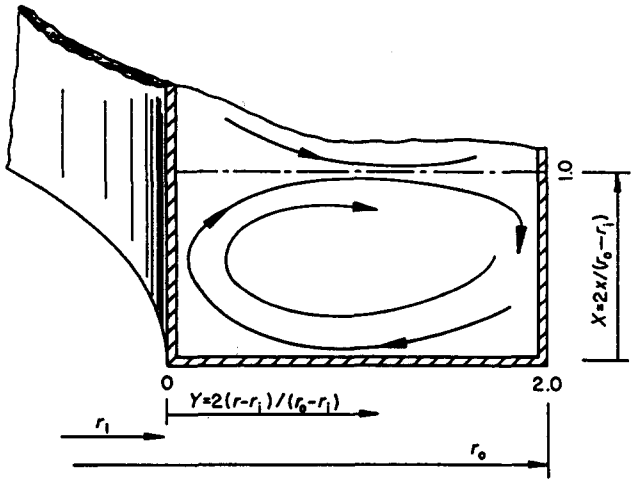

Fig 3 Describing co-ordinates and classical secondary flow pattern

following entry to the bend. To clarify the thermal data, a brief resumé will be given of the flow field results of Chang *et al*[1]. The extract compiled in Fig 4 shows the variation of streamwise velocity, $W/\bar{W}$, measured from the inner to the outer curved wall along the plane of symmetry. ($\bar{W}$ is the bulk mean value obtained from orifice plate data). At $5D_H$ upstream of the bend the profile is symmetric with a shape typical of turbulent duct flow approaching full development. At the inlet to the bend (3°) the peak velocity shifts towards the inside of the bend due to the flow acceleration on the inside and deceleration on the outside that, from inviscid flow considerations, must accompany the establishment of flow in a curved arc. At 45°, however, the velocity has shifted to the outer half of the flow due to the development of a strong secondary flow of the type shown in Fig 3. At 90° a major new feature is the appearance of a 'hole' in the axial velocity about one third of the way across the duct. It will be seen later that this low-velocity region is associated with a modification of the simple cellular secondary flow pattern of Fig 3. As the flow continues to develop around the second half of the bend, the 'hole' diminishes in magnitude and by 177° is reduced to a ripple in the velocity profile. As the flow exits from the bend the flow near the inner (convex) wall encounters an adverse pressure gradient while that near the outside of the bend is accelerated, thereby producing a nearly uniform pressure over the cross-section associated with quasi-parallel flow. This development helps keep the shear stress on the inside of the bend low and that on the outside high even though the level of secondary flow falls rapidly on exit. The peak of maximum velocity thus remains substantially displaced towards the outside wall.

The corresponding streamwise turbulence intensities are shown in Fig 5. Points to notice are: the initially symmetric profile ($-5D_H$); the strong increase in turbulent velocity fluctuations near the concave wall and their significant reduction near the inner convex surface at 45° (similar to that reported in the 90° bend study of Humphrey *et al*[8]); the local peak in turbulence activity in the region of the 'hole' in the mean velocity profile at 90°; the lingering effect of this peak at 130° and 177°; and the renewed strong increase in intensity near the outer wall as the flow develops in the downstream tangent. The different turbulence intensity levels near the concave and convex walls at 45° are qualitatively in line with the behaviour found in two-dimensional, mildly curved boundary layers. Mean and turbulent velocity profiles obtained in the present study at 5 diameters upstream and at 90° are compared with Chang *et al*'s data[1] in Fig 6. There is evidently a close agreement between the two sets which confirms that the more detailed Berkeley data can be used to help explain the present thermal measurements.

The temperature field data for conditions equivalent to those of the velocity profiles (ie $30D_H$ inlet) are shown in Fig 7; at each station, profiles are shown

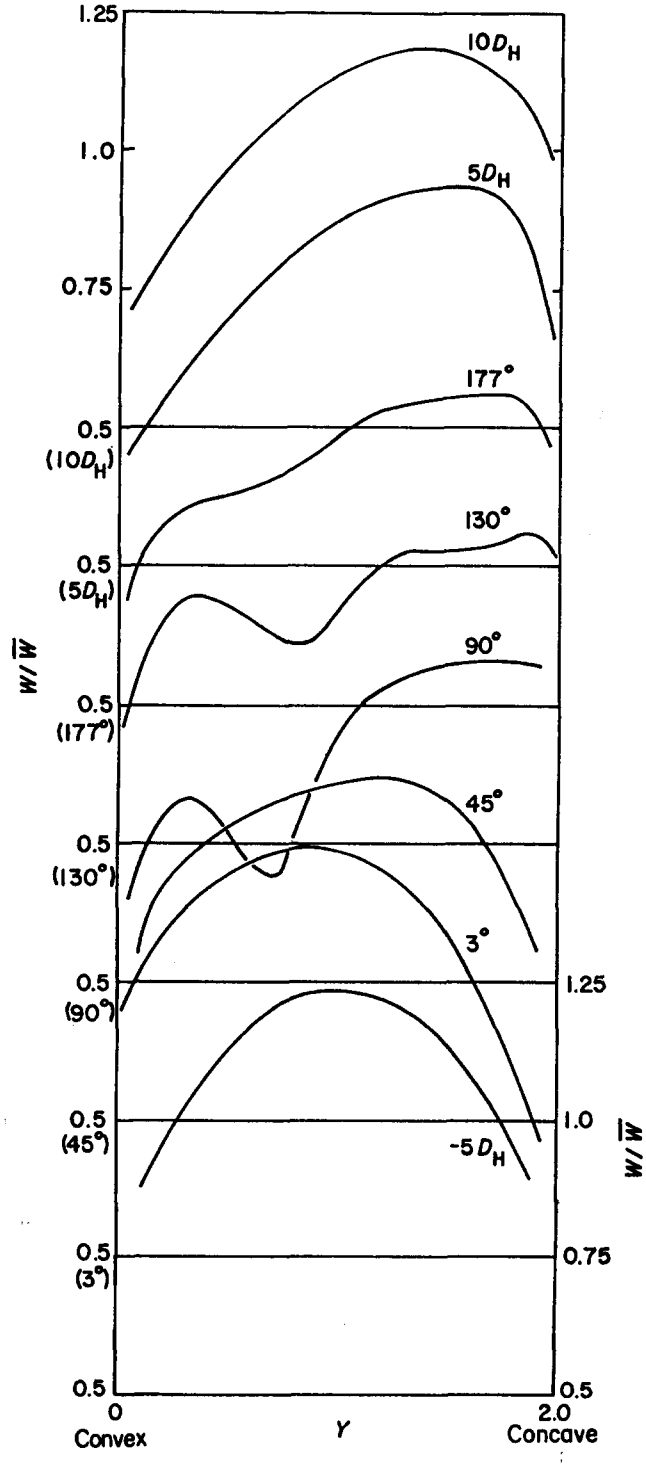

Fig 4 Development of mean velocity profile on plane of symmetry through 180° bend; data of Chang et al[1]

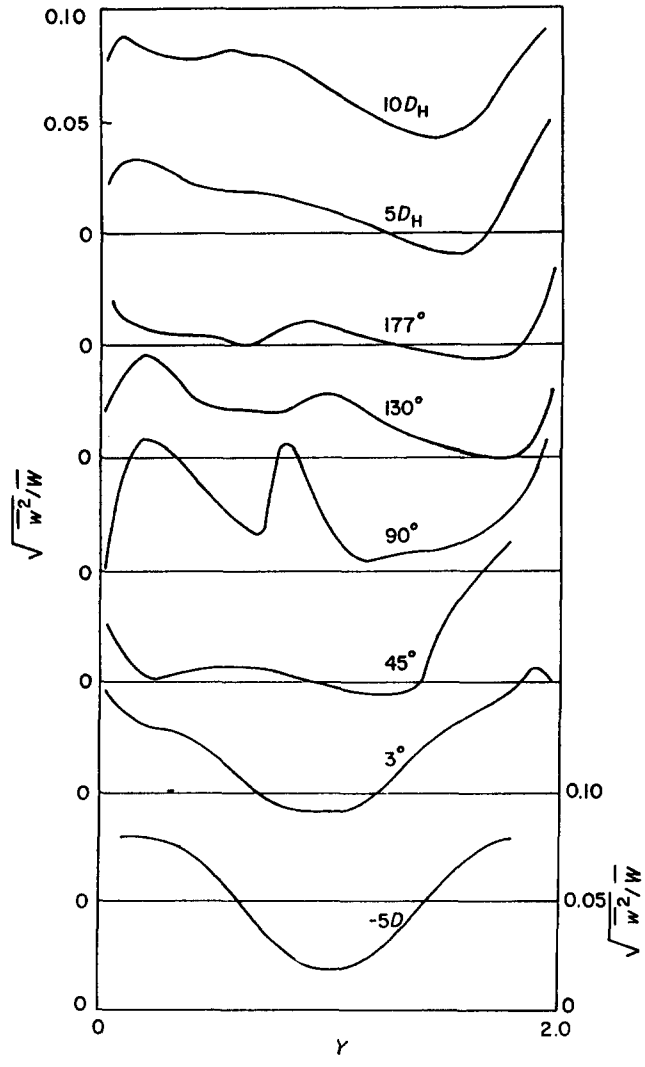

Fig 5 Development of streamwise turbulence intensity on plane of symmetry through 180° bend; data of Chang et al

along five horizontal lines ranging from the mid-plane ($X=1$) to 5.3 mm from the lower wall ($X=0.12$). The symmetric temperature profiles at $-5D_H$ become slightly skewed towards the inside of the bend at entry to the curved section. At 45° the temperatures near the convex wall are considerably higher than near the opposite wall with the minimum displaced towards the concave wall. This behaviour reflects the strongly reduced level of turbulent velocity fluctuations near the convex surface and the augmented levels near the concave wall. The effect of convective transport due to the secondary motion seems to be of rather minor importance here for (having regard for the flow pattern indicated in Fig 3) its influence would be to transport the region of minimum temperature towards the concave wall near the mid-plane and towards the convex wall for the smallest values of X. The Y co-ordinate of the minimum temperature is almost independent of X, indicating that convective transport at 45° is not a major feature.

A different picture emerges at 90° where the peaks in temperature one third of the way across the duct mimic the trough in the velocity profile. In view of the relatively high temperature of these peaks for $X=0.5$, 0.75 and 1.0, the fluid there has clearly lifted away from the convex wall (since none of the other walls is as hot as this fluid) under conditions of reduced turbulent mixing (since otherwise the temperature peak would have rapidly diffused). As with the velocity field, the peaks at 90° gradually die away over the second half of the bend, there being only a slight waviness remaining by 180°. Downstream of the band temperatures remain lower near the outer wall than the inner one, a feature that reflects the higher levels of turbulent velocity fluctuations near this surface (Fig 5). The secondary flow pattern that produces the peak in temperature at 90° can be qualitatively inferred from the isotherms map (Fig 8). The indications are that the secondary return flow near the mid-plane, which is evidently present at 45°, is brought to a halt by 90°, the return flow being thus displaced towards the lower wall. It is of interest to note that this type of behaviour has been found to occur in turbulent flow in a curved pipe of circular cross section[14].

The distribution of local heat transfer coefficients, defined as local wall heat flux divided by local difference between T_W and T_B, for this case is shown by the open symbols in Fig 9. The distributions along the three walls of the duct are presented as if the inner and outer walls had been folded down flat with the bottom wall. At $-5D_H$ (omitted for clarity) and at 0°, the levels of Nusselt number are essentially the same and exhibit nearly uniform values around the circumference†. These levels will later be seen to be consistent with what is known about heat transfer behaviour in the later stages of development of flow in square ducts. By 45° marked effects of the curvature have appeared with levels of Nu being reduced relative to entry values on the convex surface and raised on the concave wall; indeed, there is a steady diminution in Nusselt number as one proceeds around the perimeter from the centre of the concave wall to the centre of the convex wall. This behaviour is consistent with that expected from the mean temperature profiles and suggests that the intensity of turbulent fluctuations near the wall is the principal agency in affecting the heat transfer coefficient. By 90° the ratios of the heat transfer coefficients on the outside and inside has grown to a maximum level of 2.2:1 while the mean level is about 60% higher than at entry. This behaviour again seems consistent with the UC Berkeley data[1]. At 135° the heat transfer coefficients on the concave wall have begun to decrease slightly while those on the flat bottom wall have risen to nearly the same level, a behaviour that is probably due to the convection of turbulence energy by the secondary flow from near the concave wall where augmented levels are produced. At 180° a similar pattern is exhibited though the levels have begun to fall, a trend that continues into the exit tangent. Even at 9.68 diameters downstream, however, the Nu at the mid-plane of the outside wall is still 60% greater than on the inside, again probably due to the higher levels of turbulent velocity fluctuations occurring near the outer wall.

In the experiments with an entry length of $72D_H$ the mean velocity profile displays a lower ratio of maximum to bulk velocity and a higher level of turbulence intensity over the core region of the flow (Fig 6). These alterations do not have a major effect on the way the flow develops in the bend, however, for the velocity and temperature distributions at 90° shown in Figs 6 and 7 are barely distinguishable from those arising from an

† No thermocouples were placed very close to the corner where much lower levels of heat transfer coefficient are to be expected

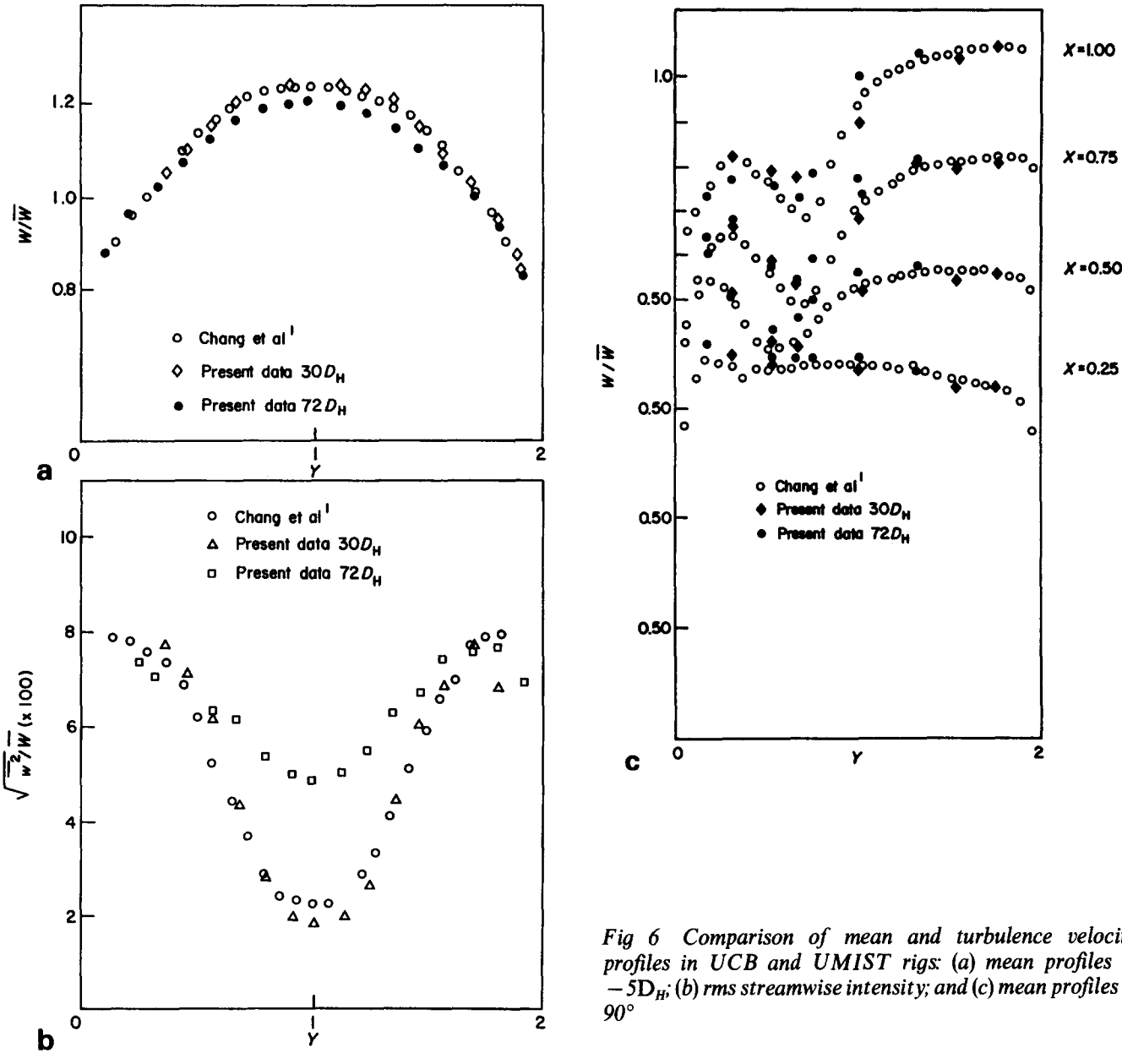

Fig 6 Comparison of mean and turbulence velocity profiles in UCB and UMIST rigs: (a) mean profiles at $-5D_H$; (b) rms streamwise intensity; and (c) mean profiles at 90°

upstream development of only $30D_H$. It is therefore not surprising to find that the only significant difference between the Nusselt number data shown in Fig 9 from those with a short entry length is in the initial region. The circumferentially averaged values of Nusselt number at $-5D_H$ and 0° are 122 and 130 respectively which are clearly higher than for partially developed flow. The former is close to the value of $Nu=120$ at $Re=56\,000$ indicated in the study by Brundrett and Burroughs[6] of fully-developed ($D_H=96$) convection in a straight, square sectioned duct. The implication of these data and our results for $30D_H$ is that, unlike developing flow in a circular sectioned pipe, the heat transfer coefficient in a square-sectioned duct falls to a minimum and thereafter rises to its fully-developed value. In fact, the predictions of Emery, Neighbors and Gessner[15] of developing flow and heat transfer in a square duct at $Re=75\,000$ do indeed show such a minimum with Nu increasing by about 17% over the region between 30 and 60 hydraulic diameters from the duct entry†. The present inlet levels of Nu are thus entirely consistent with earlier observations. At 45°, the levels of Nusselt number for the fully-developed entry are only 15% higher than for the partially developed case while by 90°, and beyond, the differences fall mainly within the limits of possible experimental uncertainty. We note, however, that in this and the subsequently reported test* the Intrex sheet had come unstuck from the concave wall of the duct in the vicinity of the 180° station so the slightly higher levels of Nu found at this position (compared with the tests with a shorter development section) should perhaps be viewed with some caution.

The corresponding behaviour for the maximum attainable Reynolds number (92 130) (but not included

† Emery *et al*[15] attribute the late rise in Nu to 'interacting shear layers' that are not present in the circular pipe flow though the cause may also be due to turbulence-driven secondary flows, which are known to develop markedly in intensity beyond $30D_H$ downstream

* But not for any of the tests with the short development length

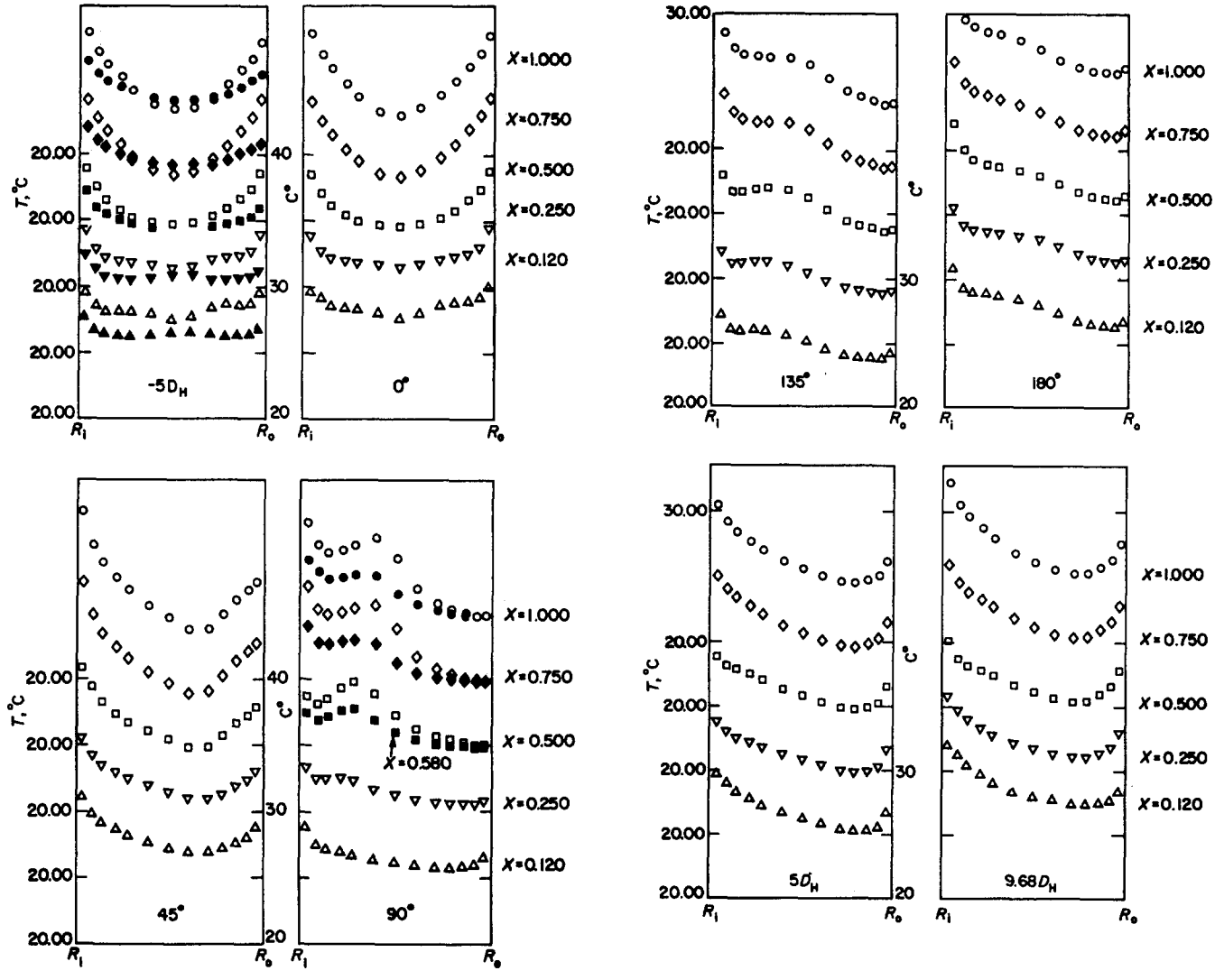

Fig 7 Mean temperature profiles at Re = *55,800 (Open symbols: 30*D_H *inlet tangent. Solid symbols: 72*D_H*(57*D_H *heated) inlet tangent*

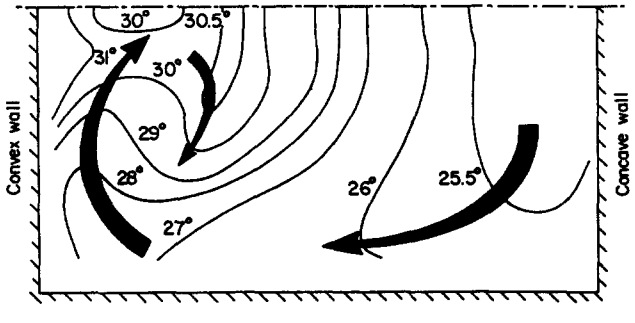

*Fig 8 Temperature contours at 90° station; 30*D_H *inlet tangent*

here[13]) accords very closely with the results described in the paragraph above. There are no significant differences in the trends or the shapes of the Nusselt number curves save that the levels of Nusselt number are higher by amounts that are consistent with the various $Nu \sim Re$ correlations for pipe flow.

For the final test at $Re = 9880$, the measured values of Nusselt number are sensitive to the assumed rate of heat loss to the surroundings in isolated regions where T_W and T_B are nearly the same‡. It is nevertheless included here because the results display some interesting differences from the tests at higher Reynolds number which, in their trends, are not affected by the greater overall uncertainty in *Nu*. Firstly, at 5 diameters upstream (Fig 10) the mean level of the Nusselt number, at 45.1, is 40% higher than indicated by the Dittus-Boelter correlation while, at the higher Reynolds numbers, this formula gave values for *Nu* that were within a few percent of those measured. We know of no previous data of convective heat transfer in a square duct at such low Reynolds number though the Brundrett and Burroughs[6] data at $Re \simeq 22\,000$ also suggest that *Nu* increases markedly relative to circular tube values as the Reynolds number is decreased. The reason for this is presumably because the level of the turbulence-driven secondary flows scales roughly on the wall friction velocity and, as the Reynolds number decreases, the friction velocity rises relative to the bulk mean value. At the inlet plane to the bend (0°) we find that the level of *Nu* has increased significantly on the inner wall due to the initial acceleration of the flow on the inside of the bend. Thereafter the convex curvature reduces the

‡ This indicates not so much that the data are imprecise but that *Nu* ceases to become a meaningful parameter

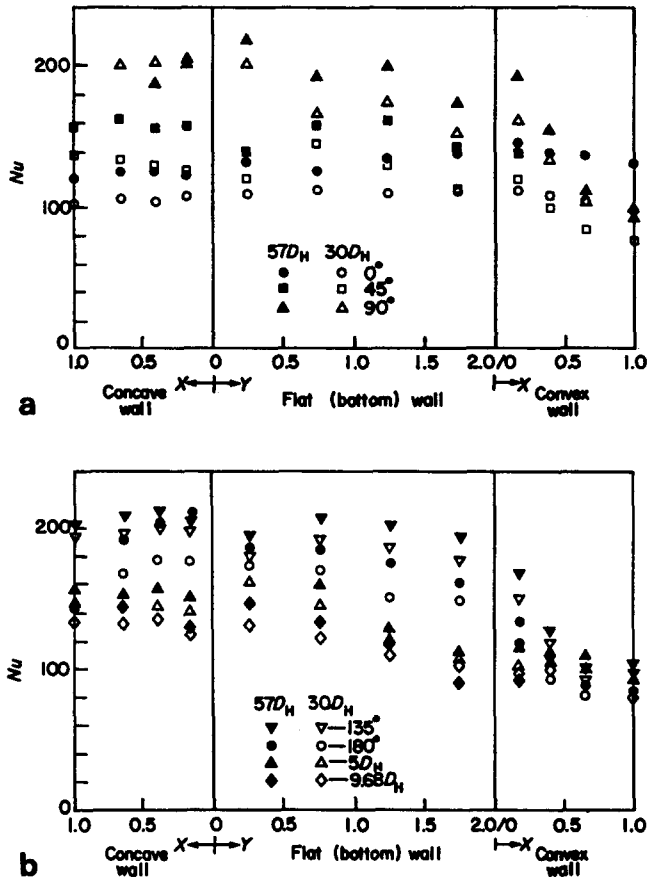

Fig 9 Local Nusselt number development in flow around 180° bend (Re = 56 030. *Inlet tangent* $30D_H$)

level of *Nu* on this surface while higher values are produced on the outer and bottom walls. By 45° the ratio of maximum to minimum levels of *Nu* exceeds 3 (compared with about 1.8 at the higher Reynolds numbers). This greater variation is qualitatively to be expected. At lower Reynolds numbers the thermal resistance of the turbulent fluid is greater than at high *Re*; so, for a given percentage change in resistance due to streamline curvature (positive on the concave wall, negative on the convex) a larger change in *Nu* will be produced. There is, moreover, a distinct change in the distribution of *Nu* on the concave wall, the highest level of heat transfer coefficient at every station occurring at the point nearest the corner, with a monotonic decrease between the corner and the centre plane being indicated. The results suggest a significantly different flow structure exists near the concave wall than at higher Reynolds numbers. Such an eventuality is not difficult to accept. A six-fold reduction in Reynolds number from the data of Fig 9 will produce an appreciable change in the axial velocity profile at entry to the bend. Since it is the non-uniformity in the streamline velocity that drives the secondary flow, the secondary flow pattern can be expected to change. The 90° bend studies at Imperial College[8-10] give a clear indication of the sensitivity of the flow structure near the concave wall to the state of the entering flow and the radius of curvature.

The thermocouple on the bottom wall closest to the corner indicates an implausibly high value of *Nu* at 90° (and to a lesser extent at 135°) due, we believe, to an underestimate in the local rate of heat loss to the surroundings. Nevertheless, the heat transfer coefficient at this near-corner position is undoubtedly higher than elsewhere on the perimeter, a feature that is consistent with the increase of *Nu* towards the corner on the concave wall discussed above. Finally, we note that the reversion, downstream of the bend, of heat transfer coefficients towards fully-developed levels appears to be taking place more rapidly at this lowest Reynolds number.

Concluding remarks

The experiments provide extensive data of convective heat transfer in a configuration for which the velocity field is already well mapped. The internal consistency of the thermal measurements appears to be good and the present data align well with the velocity and turbulence data of Chang *et al*[1]. Indeed, in some respects the heat transfer data have helped clarify the physical mechanisms at work in ways that were not possible from the velocity field data alone. For example, the near-wall behaviour on the curved surfaces over the first 45° of development seems to owe much more to curvature effects on the turbulence structure than on the induced secondary flow. At 90°, however, the isotherms suggest that the return secondary flow near the mid plane is blocked causing hot (slow moving) fluid lifted off the convex wall to curl out in a mushroom-like billow.

It is rather surprising that the ratio of heat transfer coefficients on the concave and convex surfaces is not

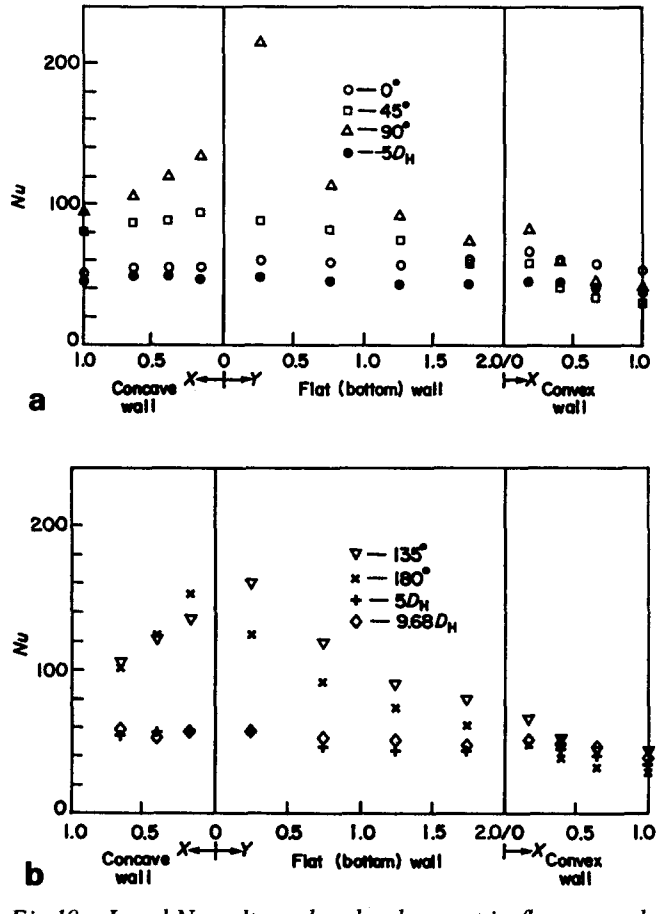

Fig 10 Local Nusselt number development in flow around 180° bend (Re = 9880. *Inlet tangent* $72D_H$ ($57D_H$ *heated*). *Assumed heat loss 8.0%*)

larger than it is, since Seban and McLaughlin[16] found a similar ratio of 2:1 between the outside and inside of a curved pipe with a radius ratio 15 times larger than that used here. This reaffirms that estimates of the effects of large perturbations on turbulent shear cannot be inferred by linearly extrapolating the effects of small perturbations.

The low Reynolds number experiment, with its strikingly different heat transfer pattern, raises interesting questions that can only be answered conclusively by providing a mapping of the mean and turbulent velocity field at $Re \simeq 10^4$.

Acknowledgements

The research has been sponsored by the US Office of Naval Research (Power Program) under Contracts N00014-80-C-0031 and N00014-83-G-0021. We wish to express our appreciation to ONR and particularly to the technical monitor Mr M. K. Ellingsworth for this support of our research.

The work has proceeded through the fullest possible cooperation of Professor J. A. C. Humphrey and his group at UC Berkeley. At UMIST we wish to thank Mr Dennis Cooper for expert work in building the apparatus and contributing many design improvements, Mr David Jackson for much help in obtaining instrumentation and providing guidance in its operation and Mr A. Prunty who built the dc power circuits. Special thanks are due to Professor J. W. Baughn, of UC Davis, who on two visits to UMIST provided expert advice on the use of Intrex and in thermocouple design. Mrs L. J. Ball prepared the manuscript with her customary precision.

References

1 **Chang S. M., Humphrey J. A. C. and Modavi A.** Turbulent flow in a strongly curved U-bend and downstream tangent of square cross section *Physico-Chemical Hydrodynamics 1983*, **4**, *243*

2 **Bradshaw P.** Effects of streamline curvature on turbulent flow, *AGARDograph 169, 1973*

3 **Simon T. J. and Moffat R. J.** Heat transfer through turbulent boundary layers – the effects of introduction and recovery from convex curvature, *ASME Paper 79-WA/GT-10, 1979*

4 **Gibson M. M., Verriopoulos C. A. and Nagano Y.** Measurements in the heated turbulent boundary layer on a mildly convex surface, *Turbulent Shear Flows-3, 1982, 80*

5 **Brundrett E. and Baines W. D.** *J. Fluid Mech. 1964*, **19**, *375*

6 **Brundrett E. and Burroughs P. R.** *Int. J. Heat Mass Trans, 1967*, **10**, *1133*

7 **Launder B. E. and Ying W. M.** *Proc. Inst. Mech. Engrs.* **187**, *1973*, *455*

8 **Humphrey J. A. C. and Whitelaw J. H.** *ASME J. Fluids Eng. 1981*, **103**, *443*

9 **Taylor A., Whitelaw J. H. and Yianneskis M.** *ASME J. Fluids Eng., 1982*, **194**, *350*

10 **Enayet M., Gibson M. M., Taylor A. and Yianneskis M.** *Int. J. Heat and Fluid Flow, 1982*, **3**, *221*

11 **Metzger D. E. and Larson D. E.** Use of melting point surface coolings for local convective heat transfer measurements in a rectangular channel, *ASME Paper 84-HT-23, 1984*

12 **Baughn J. W., Hoffman M. A., Launder B. E. and Takahashi R.** *J. Heat Transfer, 1984*, **106**

13 **Johnson R. W.** Turbulent convecting flow in a square duct with a 180° bend: An experimental and numerical study, *PhD Thesis, Faculty of Technology, University of Manchester, 1984*

14 **Azzola J. and Humphrey J. A. C.** Developing turbulent flow in a 180° curved pipe and its downstream tangent, *Presented at the 2nd International Symposium on Application of Laser Anemometry to Fluid Mechanics, Lisbon, Portugal, 2–4 July, 1984*

15 **Emery A. F., Neighbors P. K. and Gessner F. B.** *J. Heat Transfer, 1980*, **102**, *51*

16 **Seban R. A. and McLaughlin E. F.** *Int. J. Heat Mass Trans., 1963*, **6**, *387*

Books received

Simulation of Turbulence Models and their Applications, Volume 1 (in French), *eds J. Mathieu, D. Jeandel, B. E. Launder, W. C. Reynolds and W. Rodi*, pp 245, Eyrolles (France)

Turbulence Models and their Applications, Volume 2, *eds B. E. Launder, W. C. Reynolds, W. Rodi, J. Matthieu and D. Jeandel*, pp 440, Eyrolles (France)

Flow Visualization III, *ed W. J. Yang*, DM 228, $95.00, pp 903, Hemisphere/Springer-Verlag

Fundamentals of Flow Measurement, *J. P. DeCarlo*, £41.70, pp 284, Instrument Society of America (distributed by John Wiley)

Turbulent Shear Flows—4, *eds L. J. S. Bradbury, F. Durst, B. E. Launder, F. W. Schmidt and J. H. Whitelaw*, DM168, pp 403, Springer-Verlag

Principles of Turbulent Fired Heat, $69.95, pp 360, Gulf Publishing

Reference book on the mechanisms of fired heat and its optimization, from the stand-points of industrial applications in combustion, energy efficiency and emission control. Written by engineers at the French Petroleum Institute, the book discusses liquid and gaseous fuels only.

Corrosion and Deposits from Combustion Gases (abstracts and index), *ed J. E. Radway*, $95.00, pp 575, Hemisphere

Measurement Techniques in Heat and Mass Transfer, *eds R. I. Soloukhin and N. H. Afgan*, $84.50, pp 569, Hemisphere

Inclusion of a title in this section does not preclude subsequent review.